Cambridge University Press
9780521749923 – Planetary Tectonics
Thomas R. Watters and Richard A. Schultz
[Plate Section]

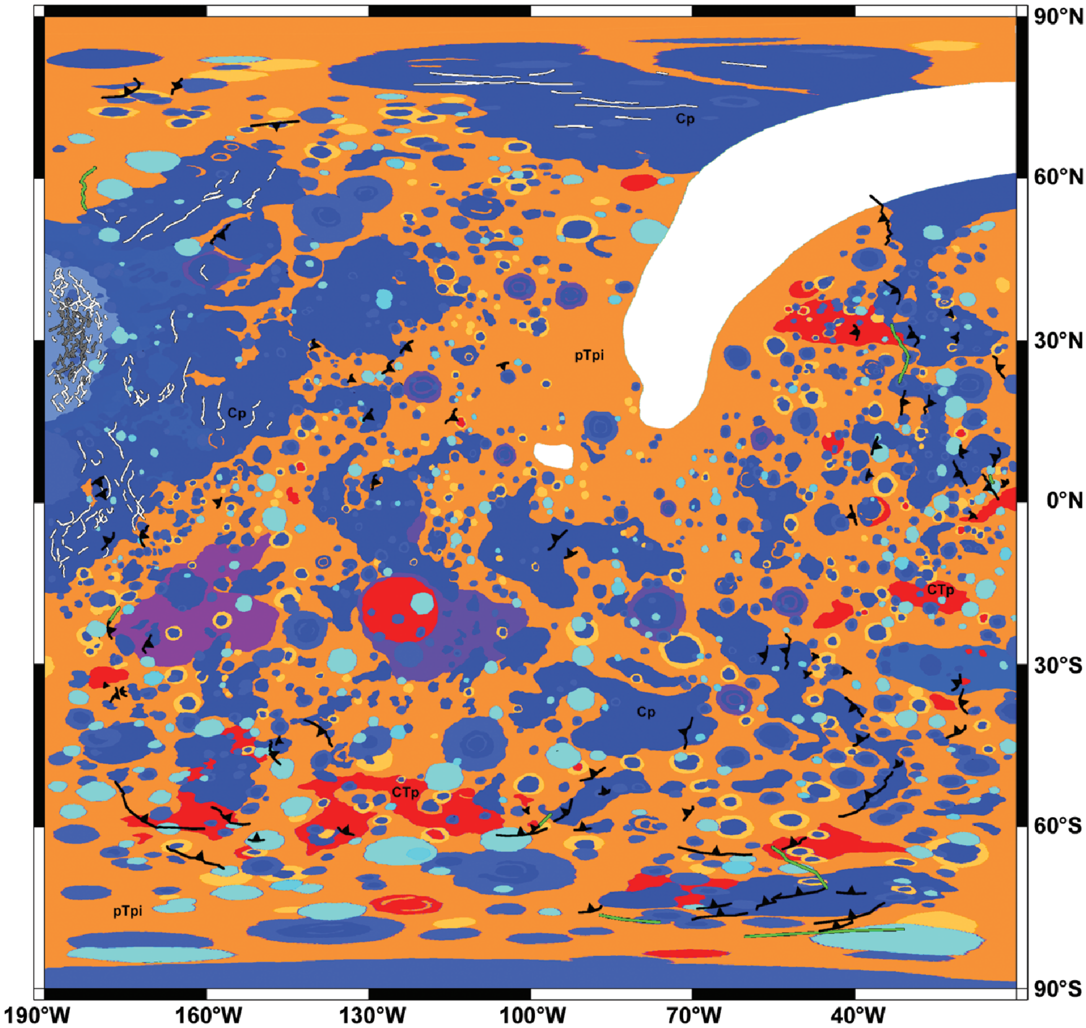

Plate 1. Tectonic features on Mercury imaged by Mariner 10. Digitized segments of lobate scarps (black), wrinkle ridges (white), high-relief ridges (green), and troughs (gray) are overlaid on the geologic map of Mercury (Spudis and Guest, 1988). The major geologic units are intercrater plains material pTpi (tan), Calorian–Tolstojan plains material CTp (red), and Calorian plains material Cp (blue). The inferred dip directions of thrust faults underlying lobate scarps are indicated by black triangles.

Cambridge University Press
9780521749923 – Planetary Tectonics
Thomas R. Watters and Richard A. Schultz
[Plate Section]

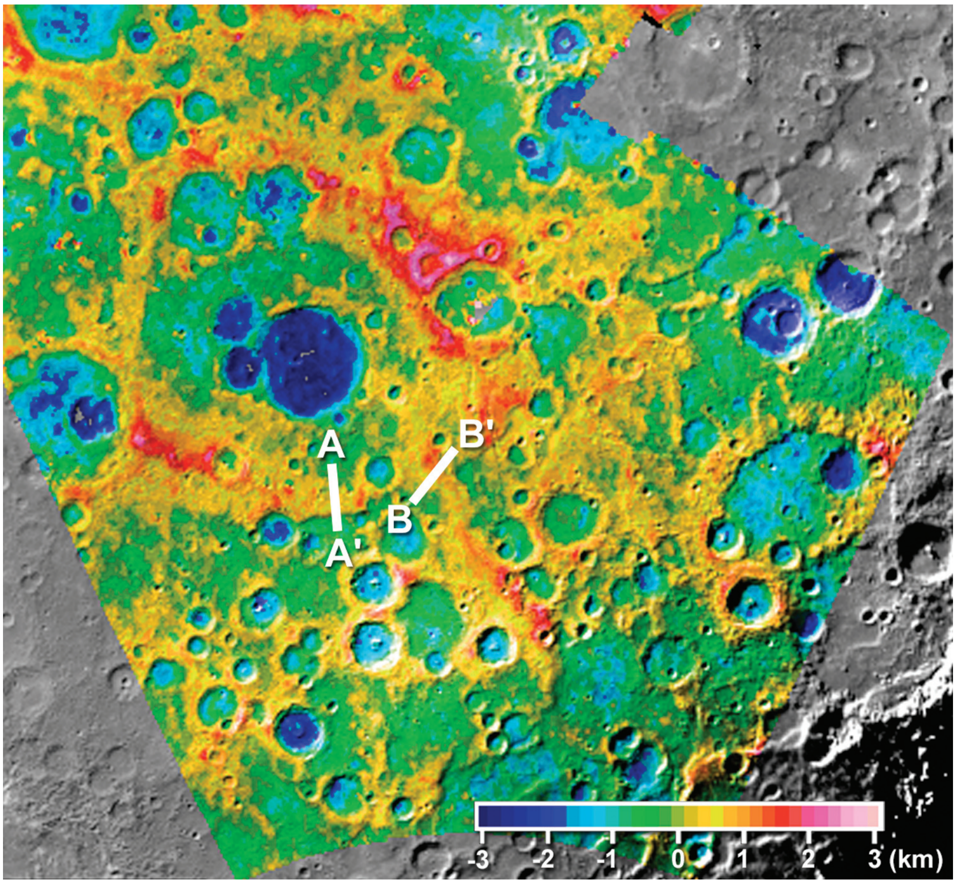

Plate 2. Regional-scale DEM generated using Mariner 10 stereo coverage overlaid on the photomosaic of Discovery Rupes, Adventure Rupes, Resolution Rupes and Rabelais Dorsum. Shades of cyan to dark blue are lows, and shades of red to pink are highs. Elevations are relative to the 2439.0 km Mercury radius reference sphere (Watters *et al.*, 2001).

Cambridge University Press
9780521749923 – Planetary Tectonics
Thomas R. Watters and Richard A. Schultz
[Plate Section]

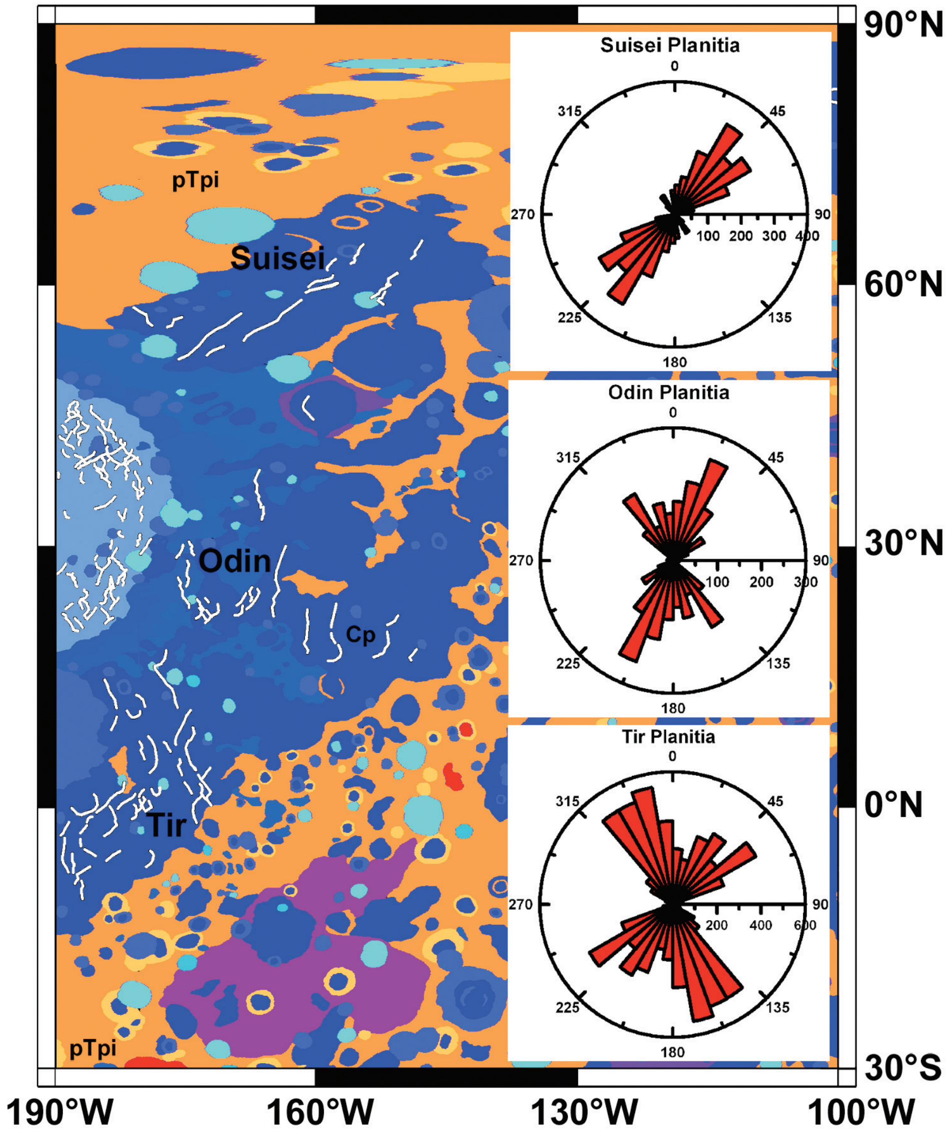

Plate 3. Rose diagrams showing the distribution of orientations of wrinkle ridges in Tir, Odin, and Suisei Planitiae. The rose diagrams are overlaid on the geologic map showing the location of mapped wrinkle ridges. Orientations are length weighted by dividing segments of constant orientation into 1 km intervals. The horizontal axes are in units of kilometers.

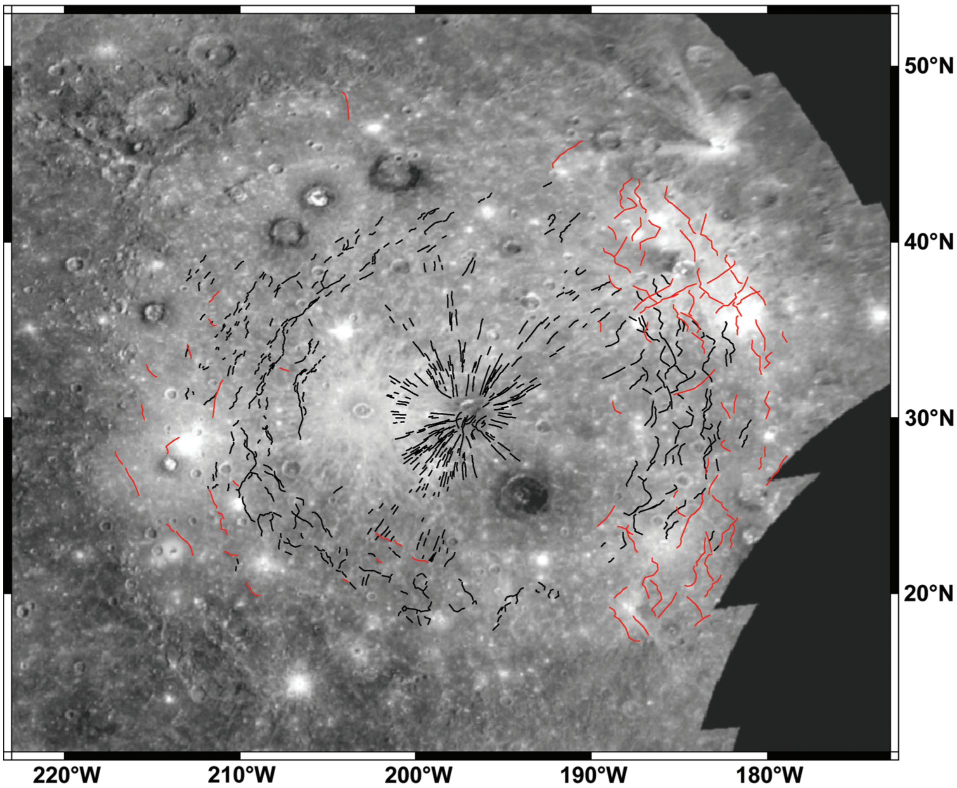

Plate 4. Map of the tectonic features of the Caloris basin. The map combines graben (560 in black) and wrinkle ridges (96 in red) digitized from MESSENGER and Mariner 10 image mosaics. The apparent gaps in the distribution and number of tectonic features between western and eastern Caloris may be due, in part, to the poor lighting geometry. Tectonic features are overlain on a MESSENGER MDIS Narrow Angle Camera high-resolution mosaic.

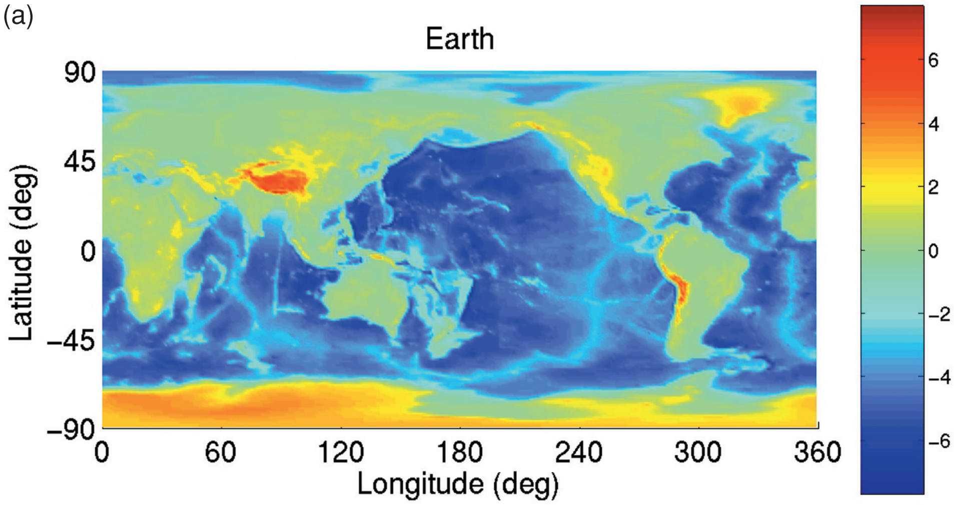

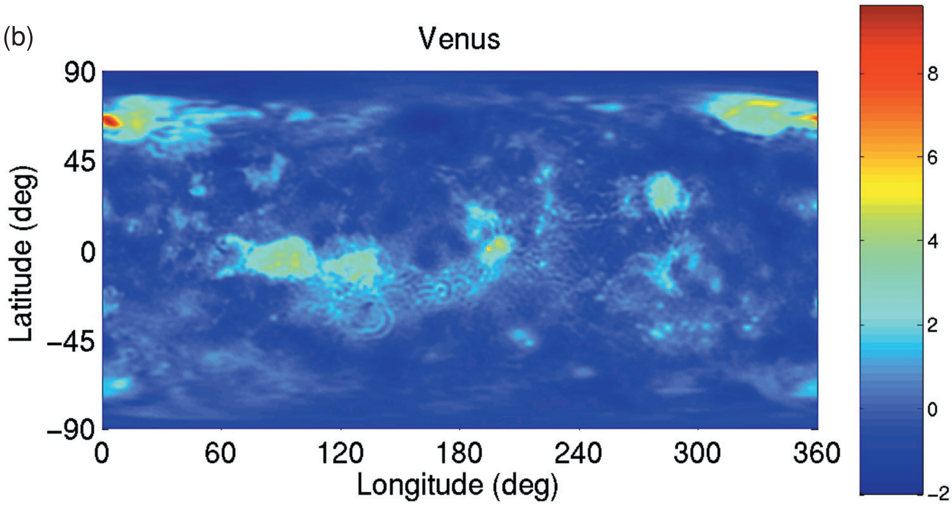

Plate 5. Topographic comparison of Venus and Earth. (a) Earth topography with "transparent" oceans; (b) Venus topography. Note prominent elevations along plate boundaries on Earth and absence of comparable plate-tectonic signature on Venus.

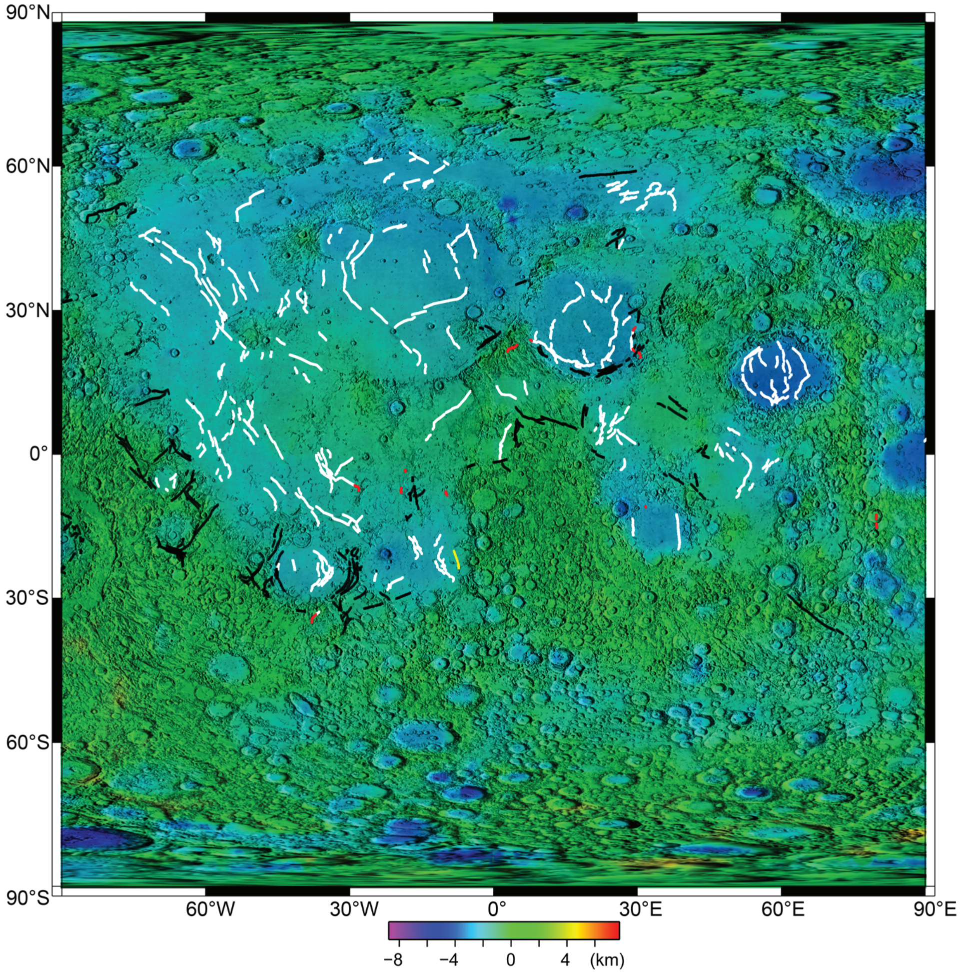

Plate 6A. Tectonic features on the nearside (A) and farside (B) of the Moon. Digitized segments of wrinkle ridges or mare ridges (white), linear and arcuate rilles (black), Rupes Recta (yellow), and lobate scarps (red) are overlaid on a shaded relief map digitally merged with color coded topographic data. The tectonic features were digitized from the digital shaded relief map. The locations of the tectonic features were checked using available Earth-based image surveys of the nearside, Lunar Orbiter images, and Apollo Metric and Panoramic camera images. The locations of features not shown on or below the limits of resolution of the shaded relief map were approximated. The topographic data is the global ULCN 2005 topographic model (Archinal *et al.*, 2006). Elevations are referenced to a sphere of 1737.4 km.

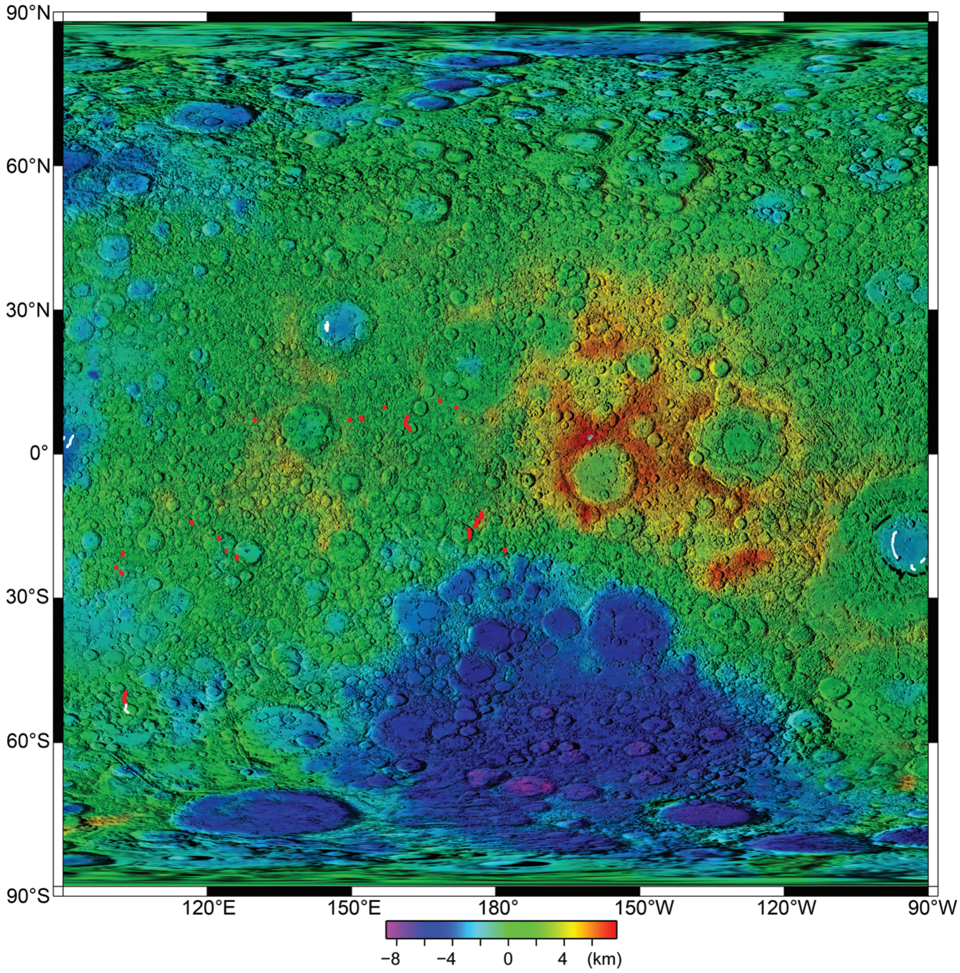

Plate 6B.

Cambridge University Press
9780521749923 – Planetary Tectonics
Thomas R. Watters and Richard A. Schultz
[Plate Section]

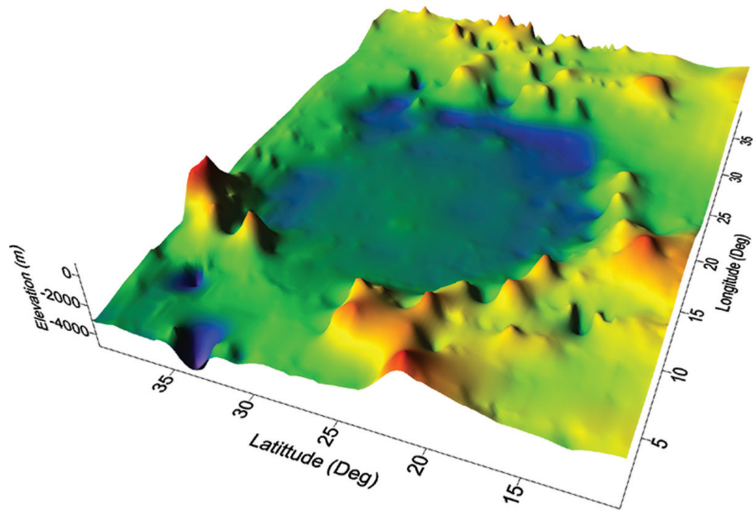

Plate 7. Topography of Mare Serenitatis. This perspective view shows that the interior of much of the Mare surface is higher than the margins. The break in slope from the interior to the margin generally corresponds to the location of the prominent wrinkle-ridge ring. The DEM was generated using Clementine LIDAR data (Smith *et al.*, 1997). Elevations are in meters above an ellipsoid of radius 1738 km at the equator with a flattening of 1/3234.93 corresponding to the flattening of the geoid.

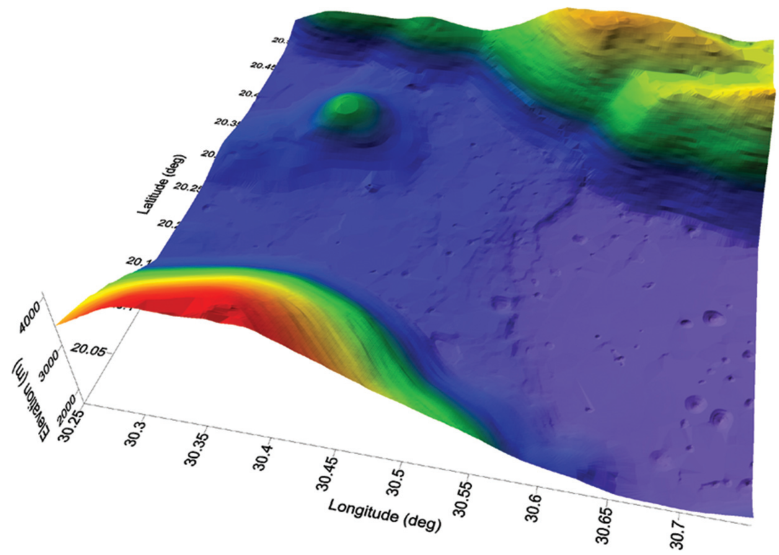

Plate 8. Digital elevation model of the Tauras-Littrow valley. The Lee-Lincoln scarp offsets the floor of the Tauras-Littrow valley by as much as 80 m. The DEM was generated by Robinson and Jolliff (2002) from a 1:50 000 scale U.S. Geologic Survey map (USGS, 1972). Elevations are relative to an arbitrary zero vertical datum.

Cambridge University Press
9780521749923 – Planetary Tectonics
Thomas R. Watters and Richard A. Schultz
[Plate Section]

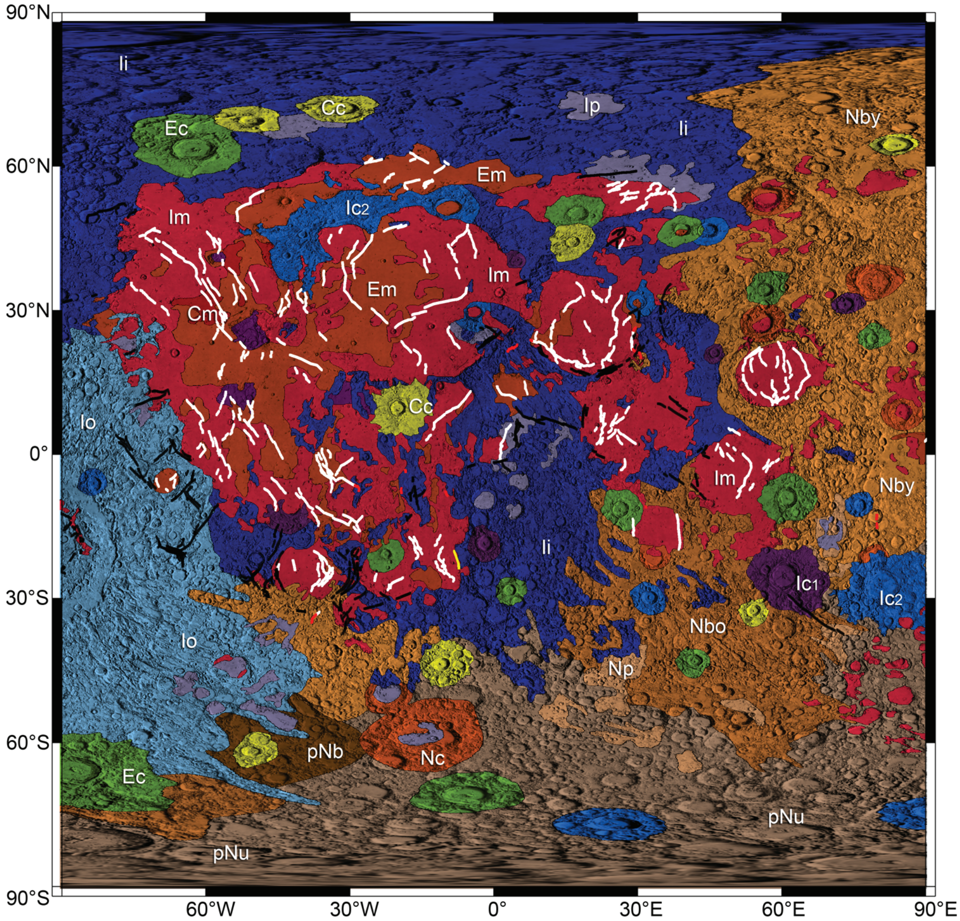

Plate 9A. Geologic map and tectonics of the nearside (A) and farside (B) of the Moon. Digitized segments of wrinkle ridges or mare ridges (white), linear and arcuate rilles (black), lobate scarps (red), and Rupes Recta (yellow) are overlaid on the geologic map of the Moon by Wilhelms (1987). The major geologic units are pre-Nectarian undivided material (pNu) and basin material (pNb), Nectarian older basin material (Nbo) and younger basin material (Nby), and crater (Nc) and plains material (Np), lower Imbrian-basin material (Ii), crater material (Ic1), Orientale-basin material (Io), and plains material (Ip), upper Imbrian mare basalts (Im), and crater material (Ic2), Eratosthenian mare basalts (Em) and crater material (Ec), and Copernican mare basalt (Cm) and crater material (Cc). For absolute ages of the lunar geologic epochs see Tanaka *et al.* (Chapter 8, Fig. 8.1).

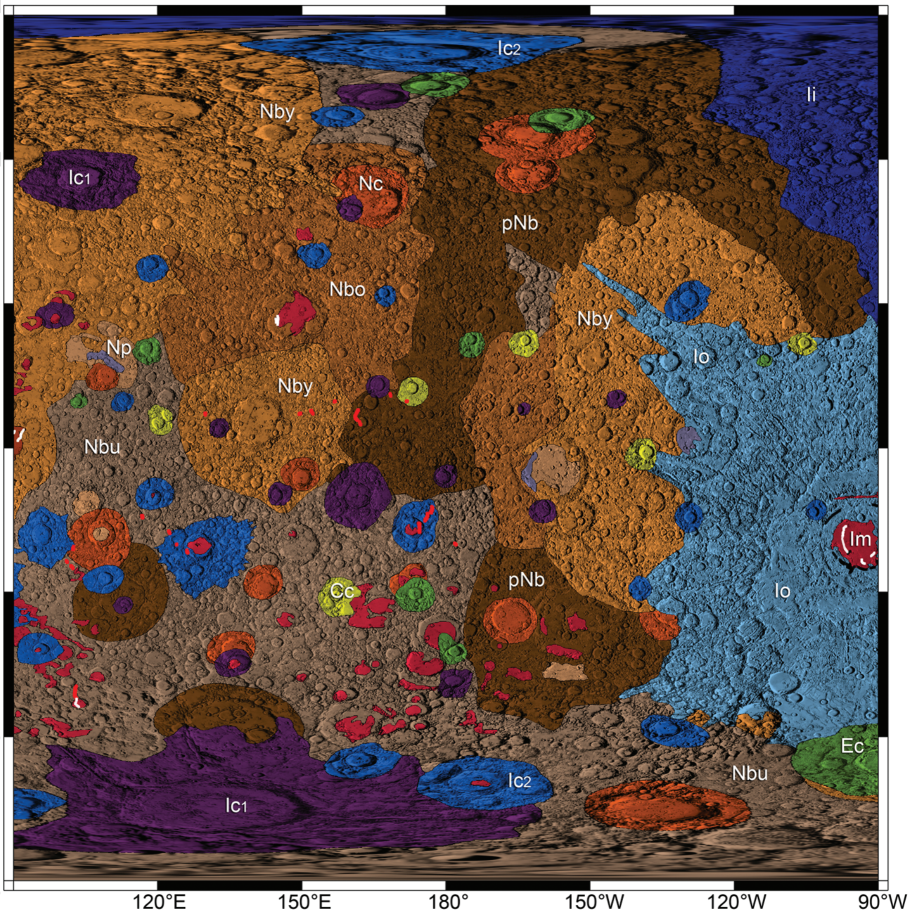
90°N
60°N
30°N
0°
30°S
60°S
90°S
120°E
150°E
180°
150°W
120°W
90°W
Ic2
Ii
Nby
Ic1
Nc
pNb
Nbo
Nby
Np
Io
Nby
Nbu
Im
pNb
Cc
Io
Ec
Nbu
Ic2
Ic1

Plate 9B.

Cambridge University Press
9780521749923 – Planetary Tectonics
Thomas R. Watters and Richard A. Schultz
[Plate Section]

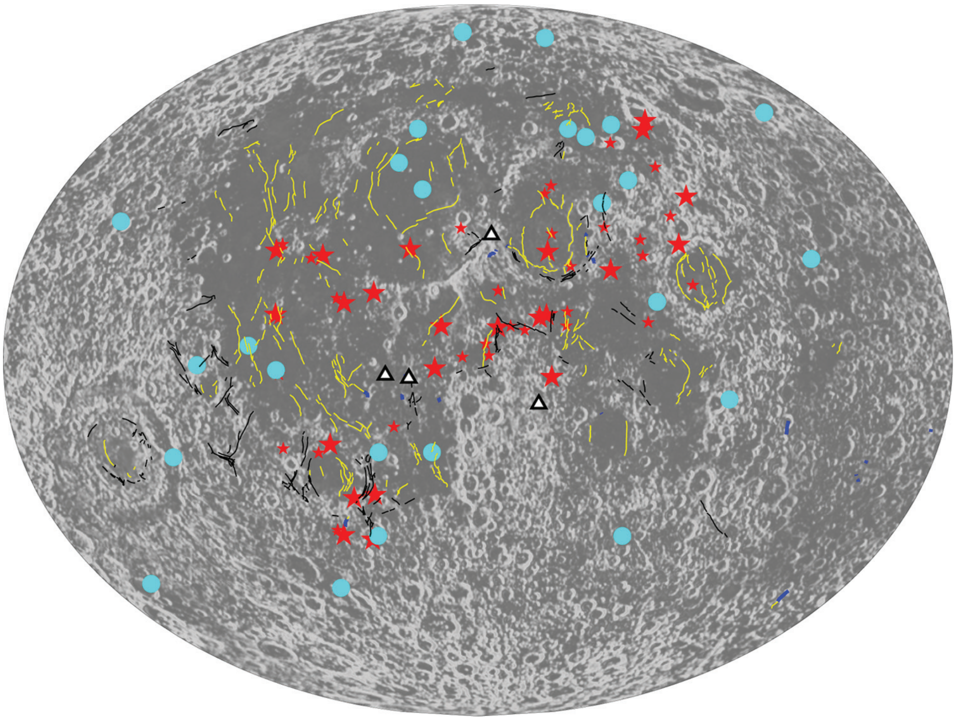

Plate 10. Shaded relief map of the lunar nearside (see Plate 5A for details) with mapped wrinkle ridges (yellow), graben (black), and lobate scarps (blue). Apollo stations 12, 14, 15, and 16 are denoted by the white triangles. Deep moonquake source region locations (red stars): 23 events from Gagnepain-Beyneix *et al.* (2006) along with the 50 events of Nakamura (2005) that have less than $\pm 10^{\circ}$ uncertainty in latitude/longitude and for which depth estimates were available. The large symbols denote the 20 clusters common to both Gagnepain-Beyneix *et al.* (2006) and Nakamura (2005), and for these events the locations in Gagnepain-Beyneix *et al.* (2006) were plotted. Small symbols are events occurring in only one of the two data sets. Turquoise circles denote the 26 shallow moonquakes located in Nakamura (1980), assuming a depth of 100 km.

Cambridge University Press
9780521749923 – Planetary Tectonics
Thomas R. Watters and Richard A. Schultz
[Plate Section]

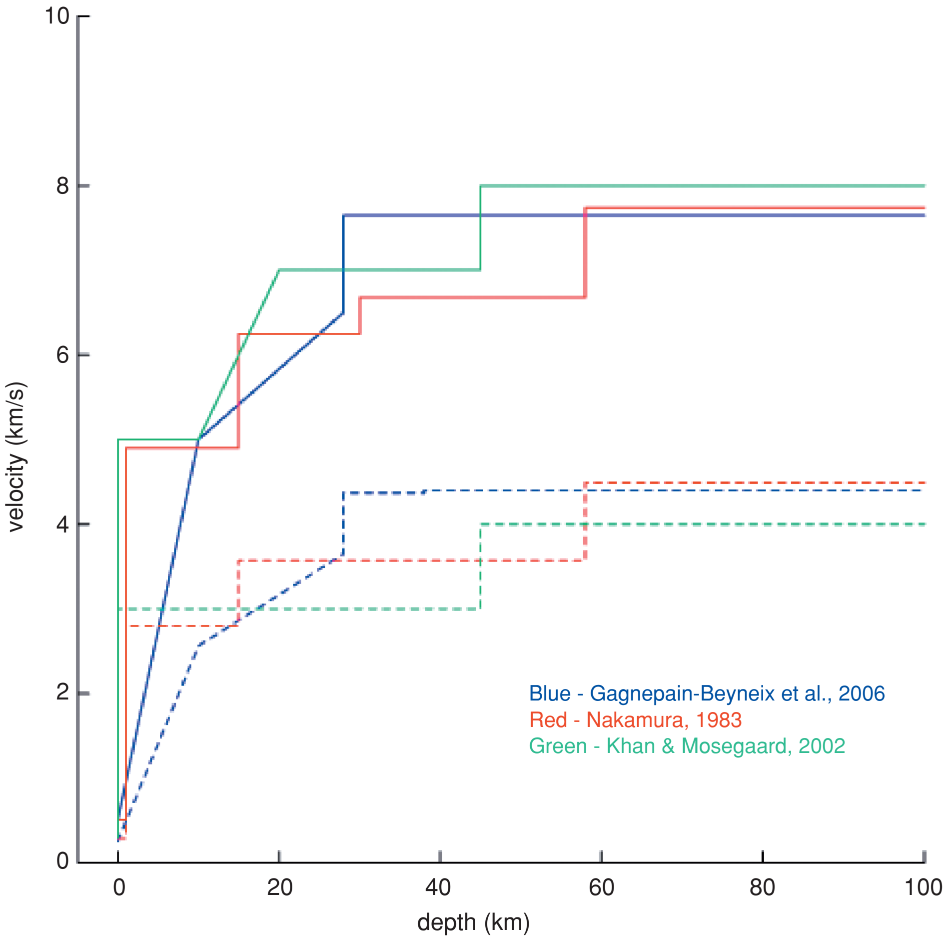

Plate 11. Seismic velocity structure of the lunar crust for three different lunar interior models: P-wave (solid) and S-wave (dashed) velocities for the three models are shown in blue (Gagnepain-Beyneix *et al.*, 2006), red (Nakamura, 1983), and green (Kahn and Mosegaard, 2002). Differences in crustal thickness among the models are seen: from 58 km (Nakamura, 1983) to 45 km (Kahn and Mosegaard, 2002) to 30 km (Gagnepain-Beyneix *et al.*, 2006).

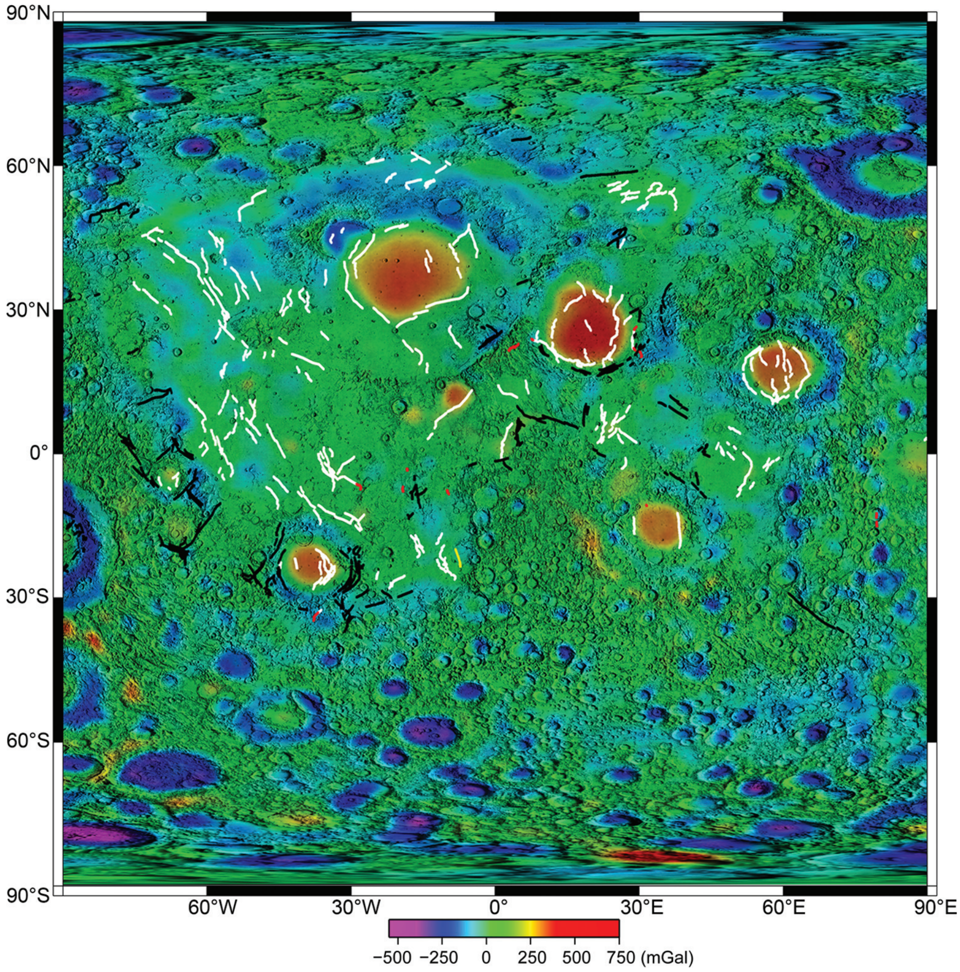

Plate 12A. Gravity and tectonics of the nearside (A) and farside (B) of the Moon. Free-air gravity derived from the Lunar Prospector LP150Q gravity model provided by Alex Konopliv, Jet Propulsion Laboratory (see Konopliv *et al.*, 2001). The grid was generated by truncating LP150Q at degree and order 140. Gravity is overlaid on the shaded relief map with digitized segments of wrinkle ridges or mare ridges (white), rilles or graben (black), Rupes Recta (yellow), and lobate scarps (red).

Cambridge University Press
9780521749923 – Planetary Tectonics
Thomas R. Watters and Richard A. Schultz
[Plate Section]

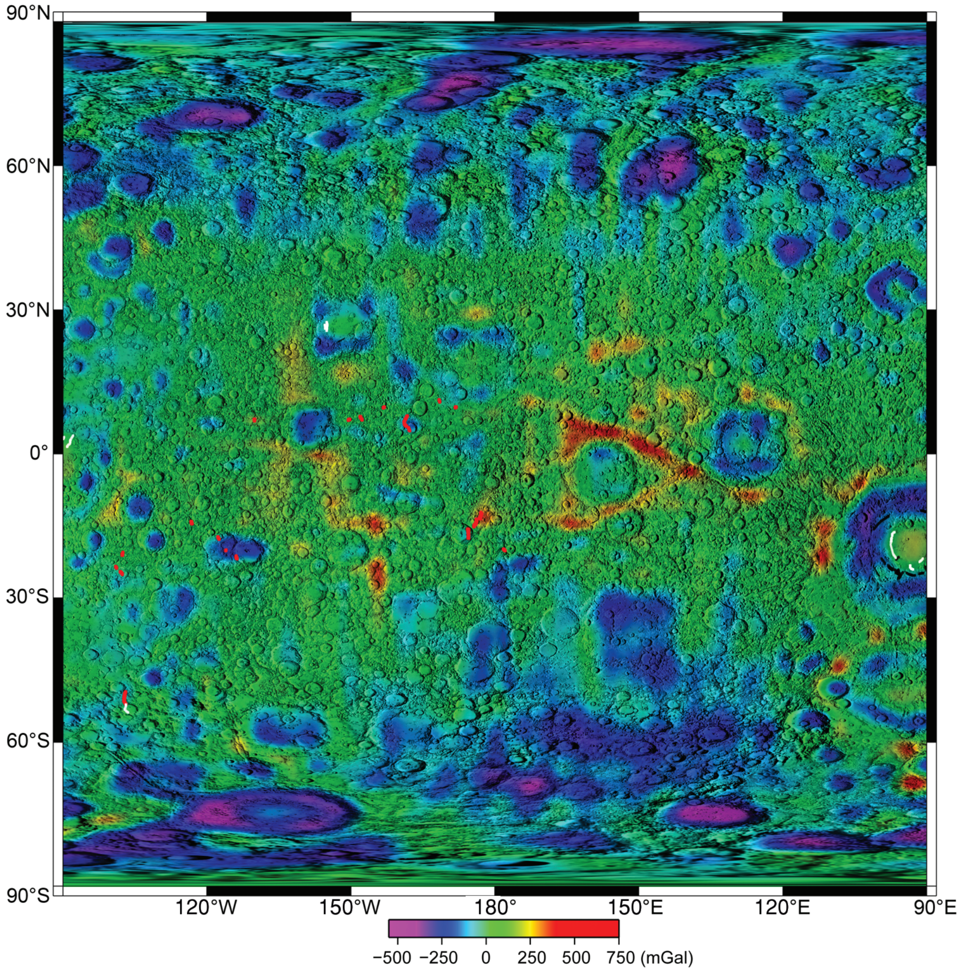

Plate 12B.

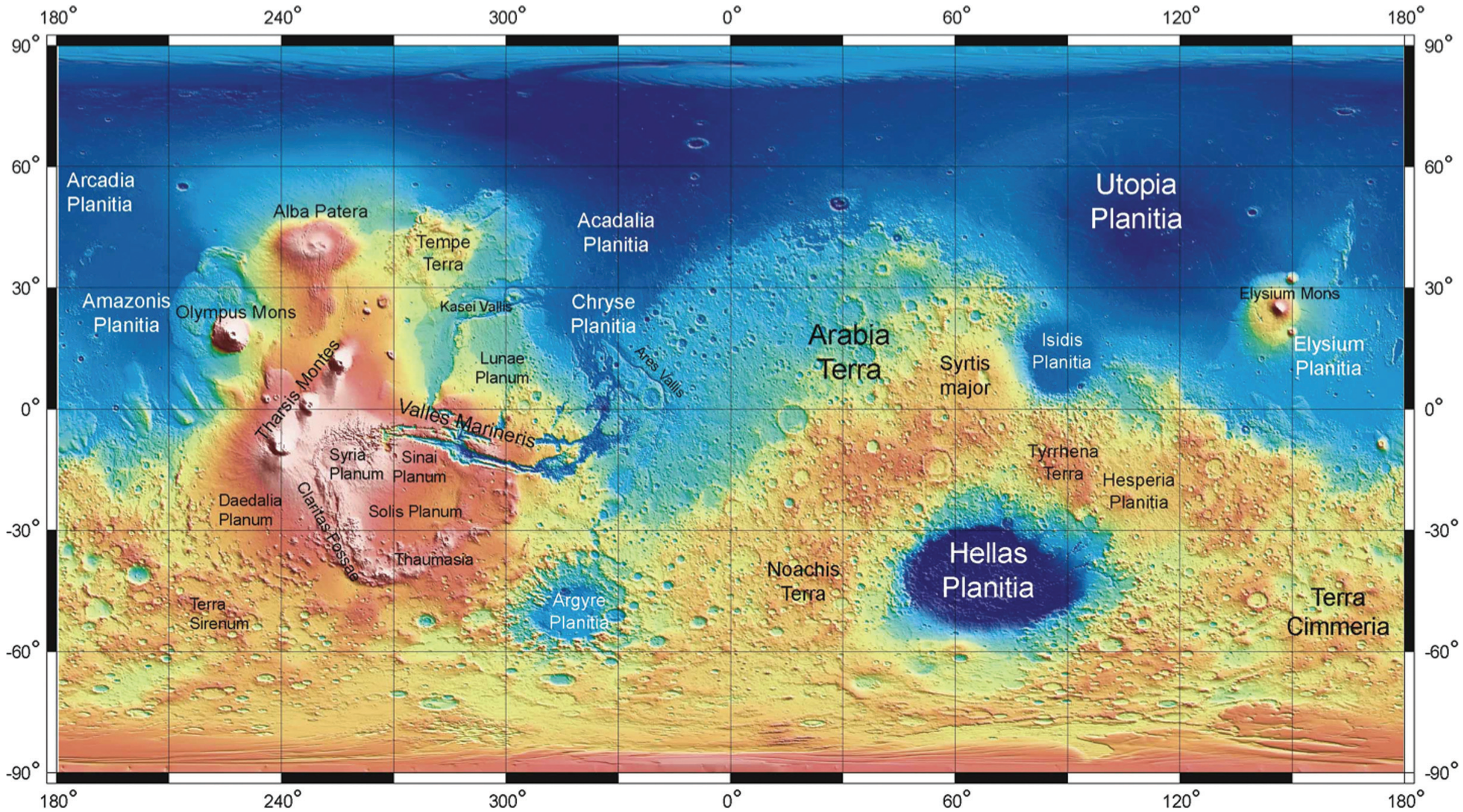

Plate 13. Topographic map and place names for Mars. The elevation range extends from ∼−8 km (blue) to ∼+8 km (light pink in Thaumasia and Tharsis rise regions). The Tharsis Montes and Olympus Mons extend to higher elevations. Simple cylindrical projection of MOLA topography.

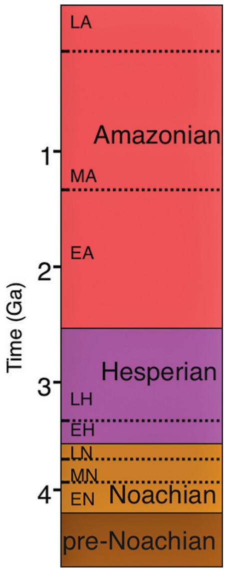

Plate 14. Geologic time scale of Mars based on major geologic/stratigraphic units exposed at the surface (Tanaka, 1986). Absolute time scale is based on correlating crater densities on Mars with radiometrically dated surfaces on the Moon (Hartmann and Neukum, 2001 and references therein; Hartmann, 2005; Tanaka and Hartmann, 2008). Within each era, epochs are shown as Early (EA, EH, EN) and Late (LA, LH, LN), Amazonian, Hesperian and Noachian, respectively. Middle Amazonian (MA) and Noachian (MN) epochs also shown.

Plate 15. Crustal thickness model (Neumann *et al.*, 2008) based on MRO spherical harmonic degree 95 gravity model 95a (A. S. Konopliv). Mean crustal thickness is 45 km and crustal density 2900 kg m^{-3}, with density adjustments made for the Tharsis volcanoes, Elysium Mons, and the polar caps.

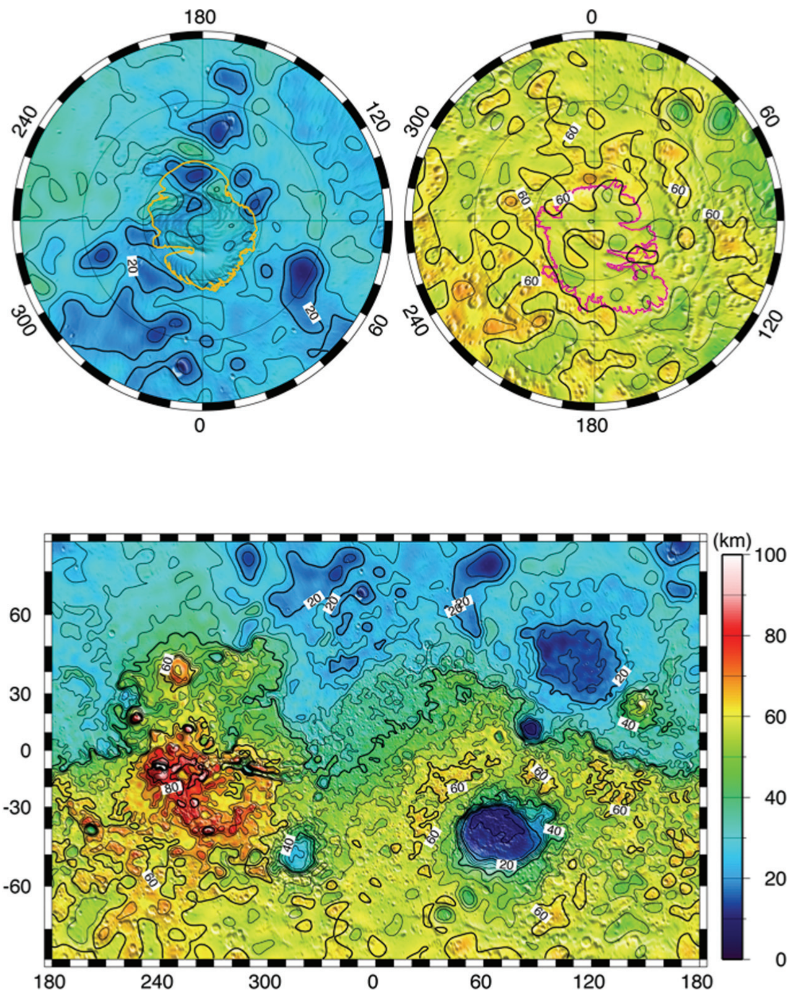

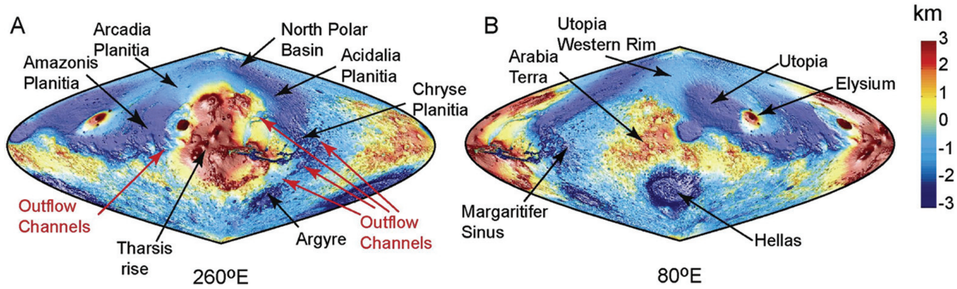

Plate 16. Observed Martian topography for hemisphere centered on Tharsis (A) and the opposite hemisphere (B). The pole-to-pole slope (the J_1 term of a spherical harmonic expansion) has been removed to emphasize other global features. A trough or moat surrounds much of Tharsis and contains most of the planet's outflow channels. To the southwest of Tharsis the trough may be obscured by both Tharsis volcanics and crustal folding. In the other hemisphere, Arabia Terra is the site of a topographic bulge. The trough and bulge are predicted by a model that localizes the Tharsis load on an elastic lithospheric shell (Phillips *et al.*, 2001). Sinusoidal projection.

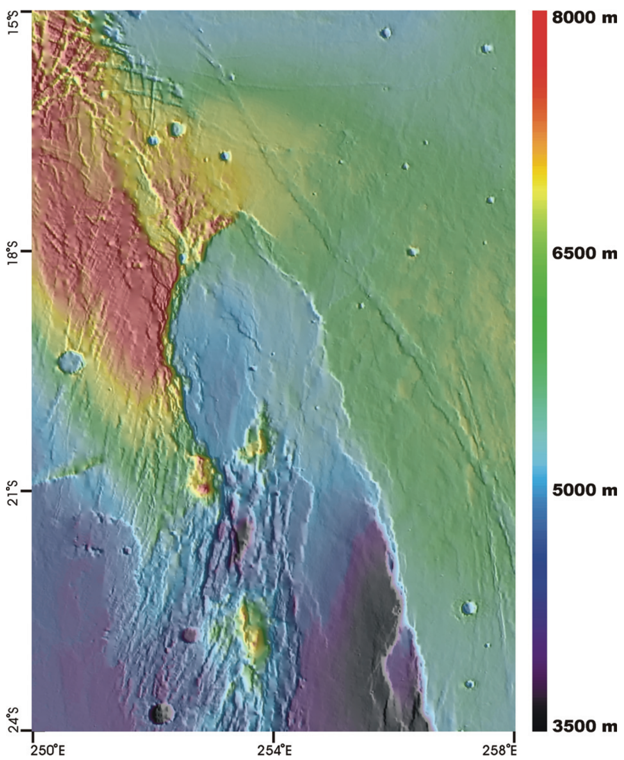

Plate 17. MOLA topographic, shaded relief map of the Thaumasia rift, analogous to a continental rift on Earth, in Claritas Fossae, Mars. The rift is 100–200 km wide with 1–2 km of relief. Note segmented nature of the rift, with the floor north of the intrarift horst tilted into the master fault on the west and the southern floor tilted into the master fault on the east. The north–northeast trending fault set is mapped as Early Hesperian in age, compared with the major rifting, which occurred in the Early Amazonian (Tanaka and Davis, 1988). The older fault set was clearly reactivated during rifting. The 360-km wide map is derived from the 0.5 km gridded MOLA elevations (Smith *et al.*, 2001), illuminated from the west.

Cambridge University Press
9780521749923 – Planetary Tectonics
Thomas R. Watters and Richard A. Schultz
[Plate Section]

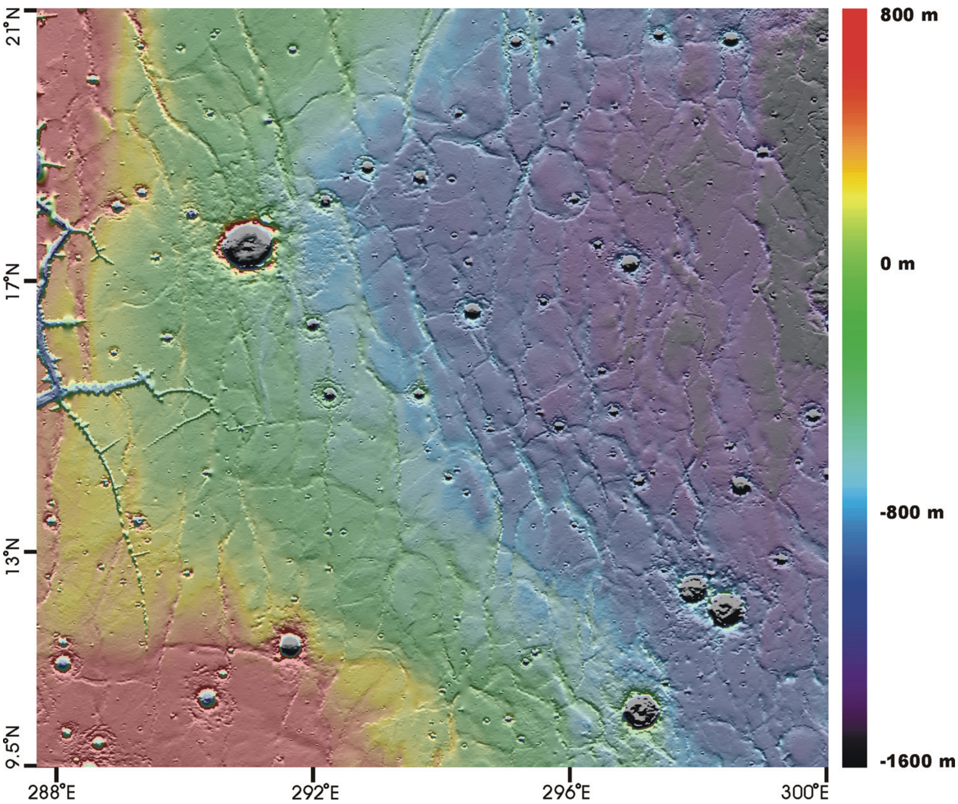

Plate 18. MOLA topographic, shaded relief map of Lunae Planum showing the classic ridged plains on Mars. Wrinkle ridges show up prominently as positive relief hills with sharper wrinkles or crenulations. The primary regularly spaced set of ridges trends generally north to north–northwest and a secondary set trends generally east–west. Note how the plains surface generally decreases in elevation to the east across wrinkle ridges (red to yellow, yellow to green, green to blue, etc.), suggesting they accommodate elevation offsets via deep-seated faulting. Subtle arches between and adjacent to many ridges can also be seen that are likely structurally related to the wrinkle ridges, but could not be seen in visible images. Ridge rings, interpreted as wrinkle ridges that follow the rims of shallowly buried craters, can be seen at 10°N, 296°E and at 18°N, 296°E. MOLA data are from the 0.5 km gridded product (Smith *et al.*, 2001), illuminated from the south. The map is 720 km wide; each degree is about 60 km.

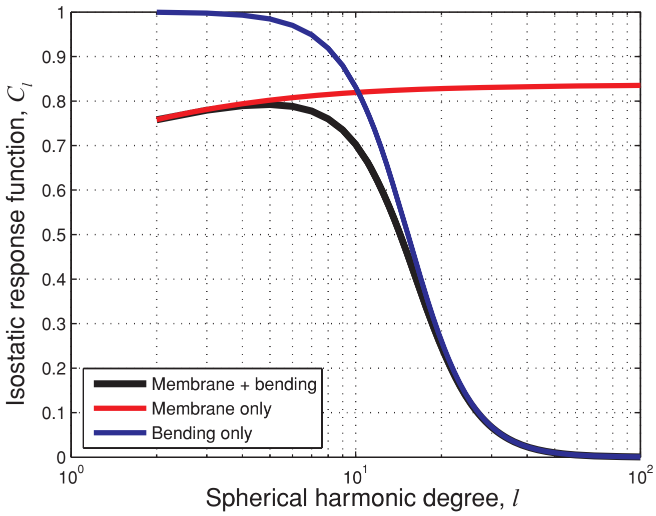

Plate 19. The "degree of compensation" or isostatic response function (Turcotte *et al.*, 1981), C_l, as a function of spherical harmonic degree, l, for a topographic load on a planetary lithosphere represented by a thin elastic spherical shell with a density contrast at its base. Perfect mass balance yields $C_l = 1$ and is possible at very long wavelengths (low spherical harmonic degree) when only bending forces are considered. The complete support of the load ("Membrane + Bending") is shown, as well as the responses obtained by isolating the membrane contribution and the bending contribution. For l less than about 10, the load is supported largely by membrane deformation. The elastic shell has a thickness, *Te*, of 100 km and a Young's modulus, *E*, of 5×10^{10} Pa. Crust and mantle densities are 2900 kg m^{-3} and 3500 kg m^{-3}, respectively.

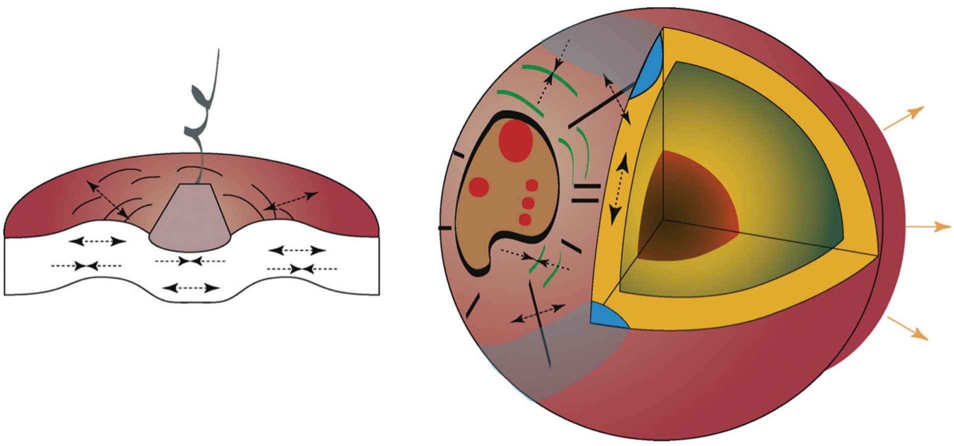

Plate 20. Stress modes on sphere and plate. Cartoon on left shows flexure on a flat elastic lithospheric plate with circumferential grabens resulting from radial extensional stresses in the flexural bulge surrounding the load. Cartoon on right indicates that for a large-scale load on a spherical elastic shell, the stress directions are switched relative to the flat plate due to the effects of membrane forces. A large load, relative to the radius of the planet, such as Tharsis, induces a trough or moat (gray) and an antipodal bulge (yellow arrows). This appears to explain the first-order gravity and topography of Mars. Outward black arrowheads indicate extensional stresses; inward black arrowheads indicate compressional stresses. Black lines and curves are graben; green curves are wrinkle ridges.

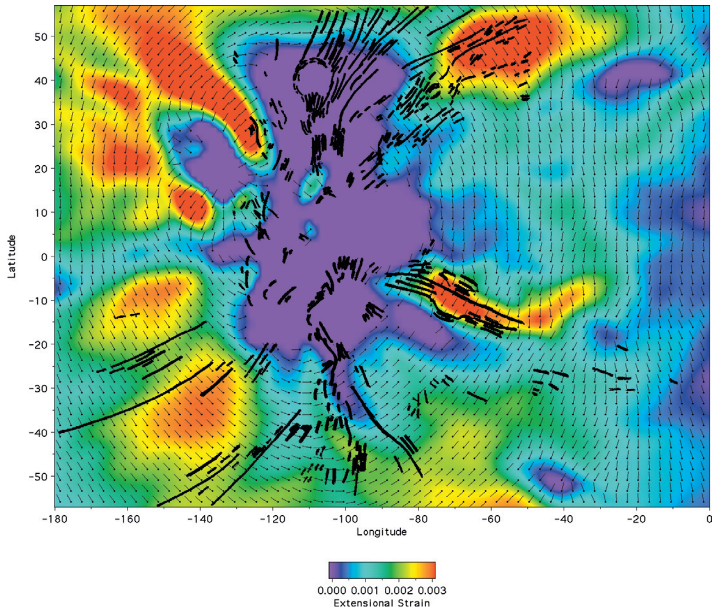

Plate 21. Extensional strain magnitude (color background) and direction (short lines) from model of elastic spherical shell loading as constrained by MGS gravity and topography data (Banerdt and Golombek, 2000). Major extensional structures are shown as heavier lines and are from Scott and Tanaka (1986). Results are shown for Tharsis (western) hemisphere. Model calculations use $T_e = 100$ km, crustal thickness = 50 km, crustal density = 2900 kg m^{-3} and mantle density = 3500 kg m^{-3}. Note structures are generally perpendicular to the extension direction, and the preponderance of structures in areas with high strain, such as Valles Marineris to the east–southeast, Tempe Terra to the northeast, Thaumasia to the south, and Sirenum to the southwest.

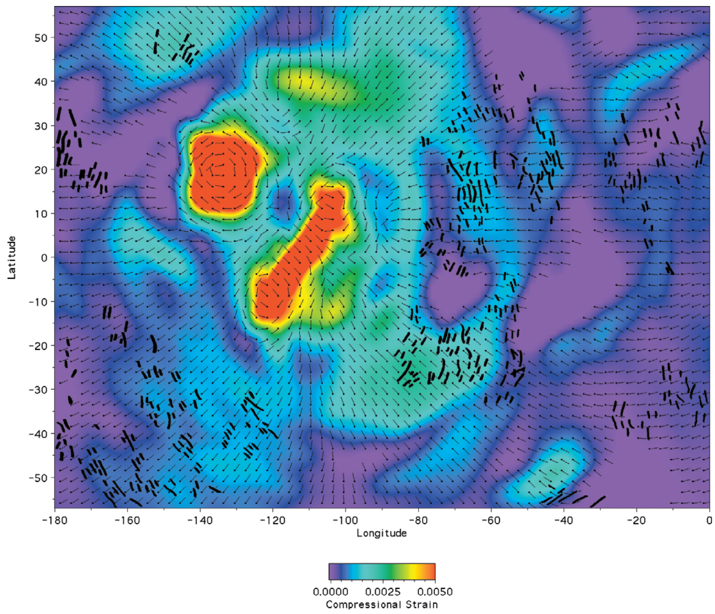

Plate 22. Compressional strain magnitude and direction from model (Banerdt and Golombek, 2000) described in Plate 21. Heavier lines are major wrinkle ridges from Scott and Tanaka (1986). Note structures are generally perpendicular to the compression direction, and the preponderance of structures in areas with relatively high strain, such as Lunae Planum to the east, Solis Planum to the southeast, Sirenum to the southwest, and Arcadia Planitia to the northwest.

Cambridge University Press
9780521749923 – Planetary Tectonics
Thomas R. Watters and Richard A. Schultz
[Plate Section]

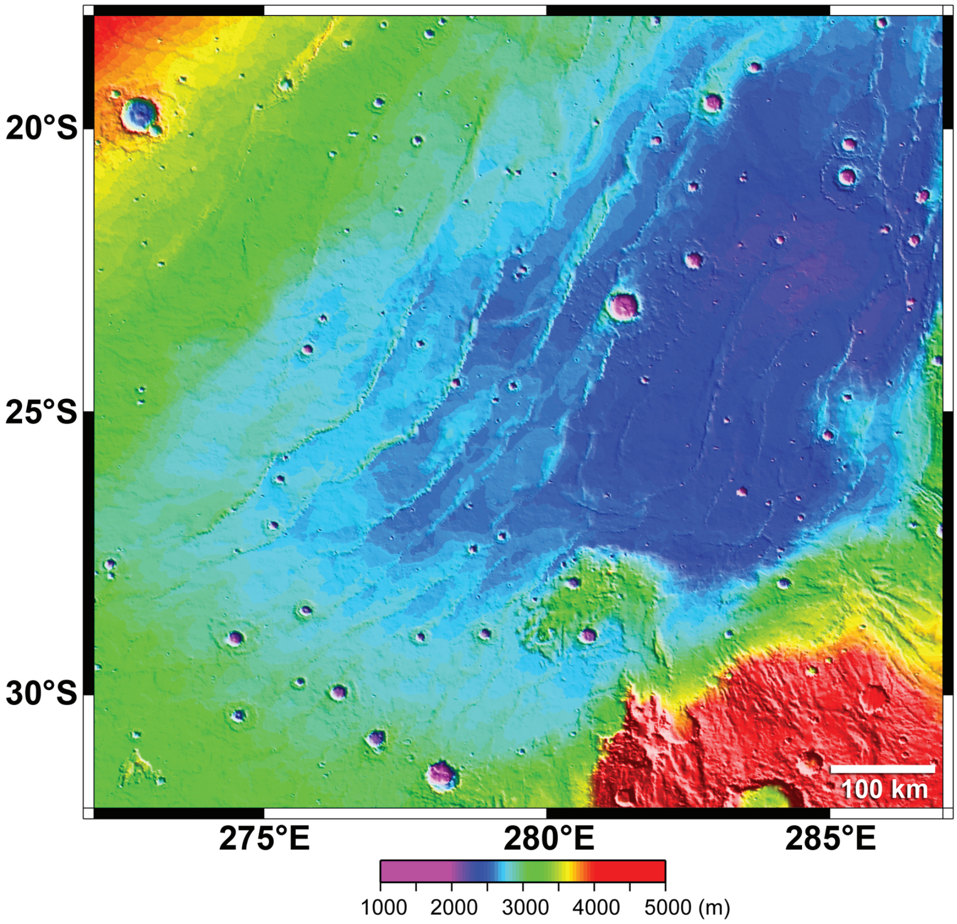

Plate 23. Ridged plains of Solis Planum, Mars. The color-coded shaded relief map generated using MOLA topographic data shows wrinkle ridges formed in ridged plains volcanic material partially filling a regional depression (see Watters, 2004). Narrow grabens and a possible rift cut highland areas at lower right. Topographic data are from the MOLA gridded 1/64° per pixel resolution model; artificial illumination from the left.

Cambridge University Press
9780521749923 – Planetary Tectonics
Thomas R. Watters and Richard A. Schultz
[Plate Section]

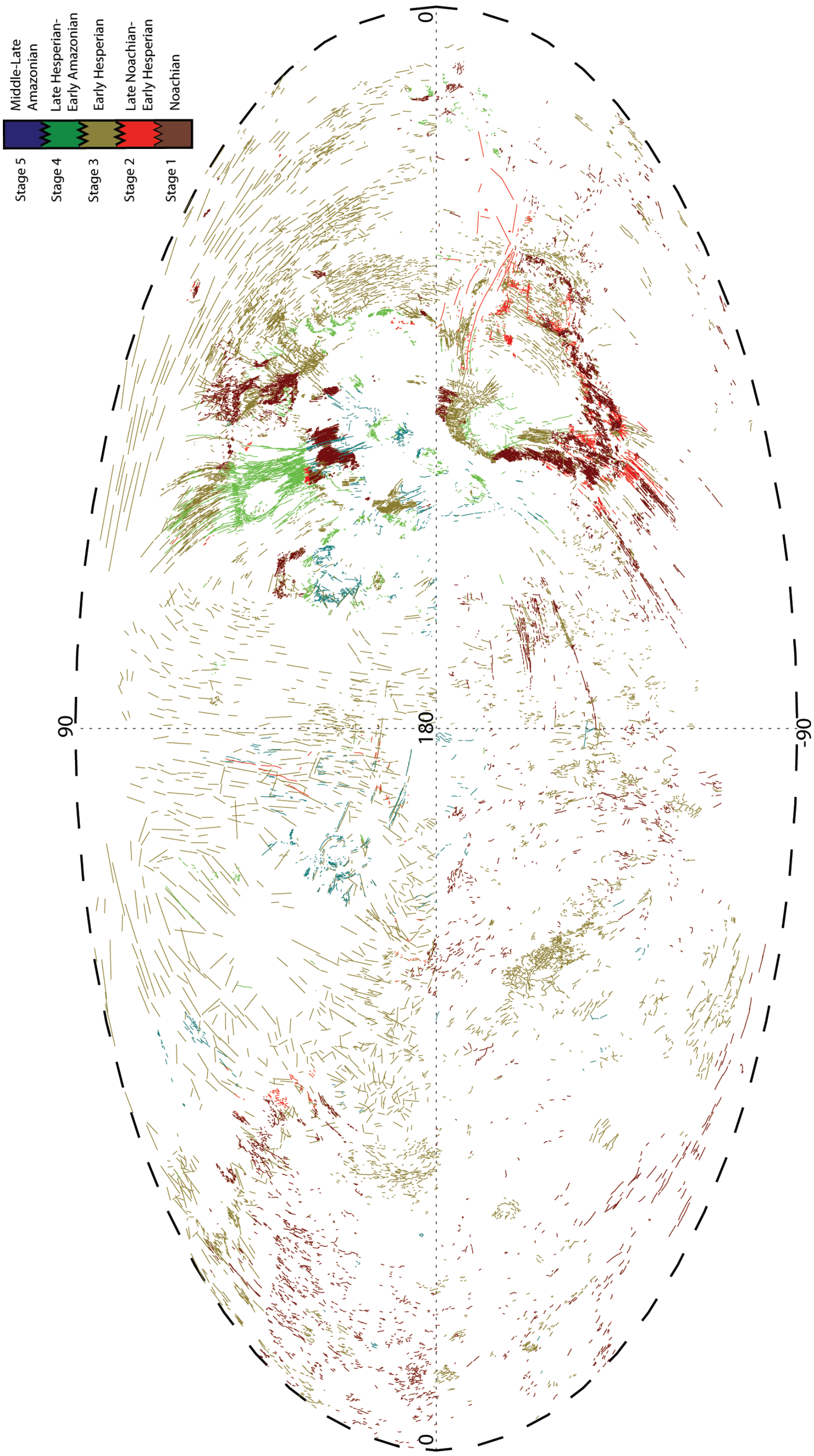

Plate 24. Map of tectonic structural features on Mars. Color coding reflects different ages of faults (grabens and wrinkle ridges) that relate to apparent major episodes of activity (adapted from Anderson *et al.*, 2001).

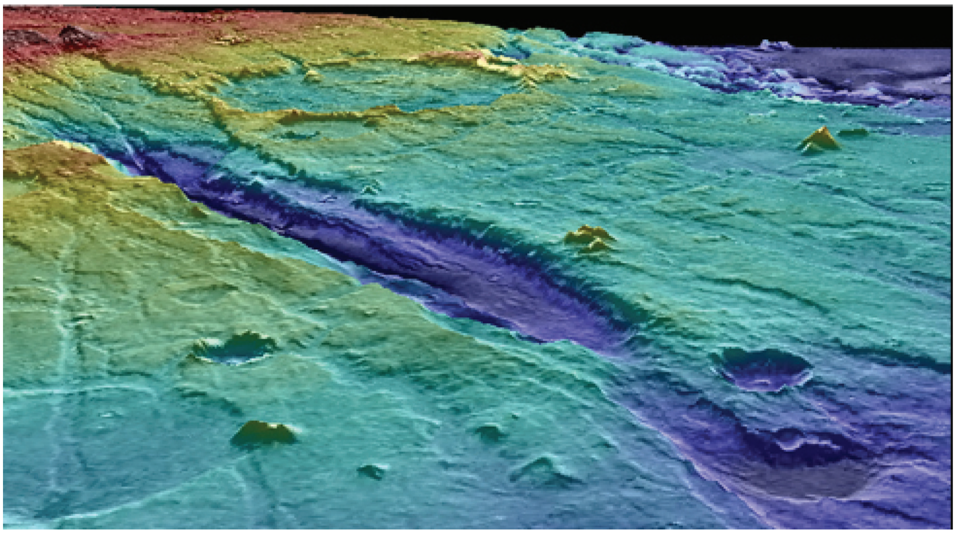

Plate 25. Oblique view of Tempe rift on Mars, looking southeast, created from MOLA DEM (Wilkins *et al.*, 2002; Okubo *et al.*, 2004). The main rift graben is ~550 km long by ~60 km wide and shows footwall uplift; many shallow grabens may represent an earlier stage of faulting in this part of northern Tharsis (e.g., Polit, 2005).

Cambridge University Press
9780521749923 – Planetary Tectonics
Thomas R. Watters and Richard A. Schultz
[Plate Section]

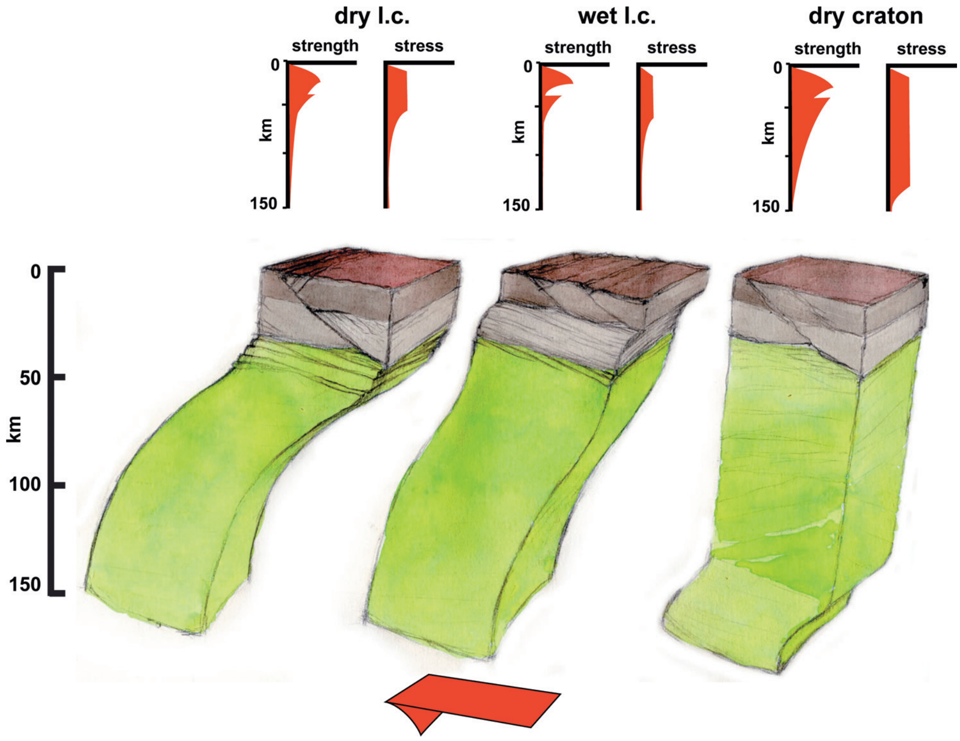

Plate 26. Cartoons illustrating generalized behavior of three regions in the Earth when subjected to shearing to the left from below. Plots showing the strength envelope and stress distribution for each cartoon are shown above. In the left cartoon, dry crust deforming predominantly by frictional sliding on faults overlies a mantle characterized by dislocation glide at shallow depths and dislocation creep below; such a cartoon may provide a reasonable approximation to oceanic lithosphere. The crustal thickness in this cartoon is exaggerated for clarity. In the center cartoon, dry upper crust overlies a weaker lower crust that deforms plastically, presumably due to water weakening; the mantle lithosphere deforms as in the left cartoon. Note that there is a weak lower crustal zone separating stiffer upper crustal and upper mantle regions (the jelly sandwich model). This cartoon might be appropriate to a back-arc setting where water released from the downgoing slab may weaken the lower crust. The right cartoon shows a possible scenario for cratonic lithosphere, where the crust overlies a stable, presumably dry, continental root. A stiff crust deforming predominantly by frictional sliding at shallow depths and localized plastic flow at greater depths overlies a stiff dry mantle lithosphere, which is underlain by wet convecting asthenosphere at depths greater than 100 km. Drawing courtesy of B. K. Holtzman.

